Revista Brasileira de Geografia Física v.18, n.07. (2025) 5406-5420.

ISSN:1984-2295

Revista Brasileira de Geografia Física

Homepage:https://periodicos.ufpe.br/revistas/rbgfe

Avaliação da expansão urbana e seu impacto na dinâmica de escoamento superficial de uma bacia hidrográfica urbana na cidade de Caruaru (PE, Brasil)

Ingrid Mariane de Oliveira Freitas[1], Luan Alves Furtado[2], José Martins de França Neto[3], Severino Martins dos Santos Neto[4], Artur Paiva Coutinho[5]

[1] M.Sc. em Engenharia Civil e Ambiental, Núcleo de Tecnologia, Universidade Federal de Pernambuco, Av. Marielle Franco; s/n; Km 59 - Nova Caruaru, CEP 55014-900; Caruaru; Pernambuco, (81)91636706, ingrid_marianeof@hotmail.com. (21)971371099 [2] Doutorando em Tecnologias Energéticas e Nucleares, M.Sc. em Engenharia Civil e Ambiental, Centro de Tecnologia e Geociências, Universidade Federal de Pernambuco, Av. Prof. Luiz Freire; 1000; Cidade Universitária, CEP 50740-454; Recife; Pernambuco, (81)993813150, luan.furtado@ufpe.br (autor correspondente). [3] Doutorando em Tecnologias Energéticas e Nucleares, M.Sc. em Engenharia Civil e Ambiental, Centro de Tecnologia e Geociências, Universidade Federal de Pernambuco, Av. Prof. Luiz Freire; 1000; Cidade Universitária, CEP 50740-454; Recife; Pernambuco, (81)998280576, jmfrancaneto@gmail.com. [4] Dr. em Tecnologias Energéticas e Nucleares, Professor Visitante, Núcleo de Tecnologia, Universidade Federal de Pernambuco, Av. Marielle Franco; s/n; Km 59 - Nova Caruaru, CEP 55014-900; Caruaru; Pernambuco, (81)91636706, martinsdsn@gmail.com. [5] Dr. em Engenharia Civil, Professor Adjunto, Centro Acadêmico do Agreste, Universidade Federal de Pernambuco, Av. Marielle Franco; s/n; Km 59 - Nova Caruaru, CEP 55014-900; Caruaru; Pernambuco, (81)991177897, arthur.coutinho@ufpe.br.

Artigo recebido em 18/05/2024 e aceito em 20/08/2025

R E S U M O

A urbanização provoca mudanças nas características originais de uso do solo, gerando significativo impacto ambiental devido ao aumento das taxas de impermeabilização e ocupação desordenada das vias urbanas. Ao longo dos últimos anos, a maior disponibilidade de imagens de satélites de média e alta resolução permitiram acompanhar a expansão urbana e seu impacto na dinâmica de escoamento superficial das bacias hidrográficas através de Sistemas de Informações Geográficas (SIGs). Dentre os centros urbanos afetados pela alta urbanização, a cidade de Caruaru-PE, apresenta uma taxa de crescimento maior que a média do Brasil, apresentando grande impermeabilização do seu solo natural, e como consequência, graves problemas de alagamentos e inundações. Neste cenário, foi realizada a classificação de imagens de sensoriamento remoto da bacia de contribuição urbana dos anos 2000, 2015 e 2020 em cinco classes: área verde, área impermeável dos lotes, via de asfalto, via de paralelepípedo e solo compactado. Os resultados apresentaram significativa redução da área verde e, quase na mesma proporção, aumento da área impermeável dos lotes, enquanto as outras classes tiveram poucas alterações. A vazão máxima de escoamento superficial, estimada pelo método racional, foi de 26% entre os anos de 2000 e 2015, e de 41% entre os anos de 2000 e 2020.

Palavras-chave: sig, método racional, scs.

Evaluation of urban expansion and its impact on the dynamics of surface runoff in an urban watershed in the city of Caruaru (PE, Brazil)

A B S T R A C T

Urbanization causes changes in the original characteristics of land use, generating significant environmental impact due to increased waterproofing rates and disorderly occupation of urban roads. Over the last few years, the greater availability of medium and high resolution satellite images has made it possible to monitor urban expansion and its impact on the dynamics of surface runoff in river basins through Geographic Information Systems (GIS). Among the urban centers affected by high urbanization, the city of Caruaru-PE, has a growth rate higher than the Brazilian average, presenting great waterproofing of its natural soil, and as a consequence, serious problems with flooding. In this scenario, remote sensing images of the urban contribution basin from the years 2000, 2015 and 2020 were classified into five classes: green area, impervious area of lots, asphalt road, cobblestone road and compacted soil. The results showed a significant reduction in the green area and, almost in the same proportion, an increase in the impermeable area of the lots, while the other classes had few changes. The maximum surface runoff flow, estimated by the rational method, was 26% between the years 2000 and 2015, and 41% between the years 2000 and 2020.

Keywords: gis, rational method, scs.

Introduction

Unplanned urban development triggers a series of modifications in the dynamics of the water cycle in the Earth's atmosphere, which under natural conditions can be considered a balanced system (Gohain et al., 2021; Ahmed; Luqman, 2024; Pereira et al., 2024). In general, disorderly urban development is associated with significant alterations in land use and occupation, resulting in reduced volumes of vegetation interception, evaporation, and infiltration, and a substantial increase in surface runoff. Furthermore, changes in land use and occupation patterns can alter the quality of both surface and groundwater, as well as aquatic ecosystems within a watershed (Menezes et al., 2016; Ferraz et al., 2022; Moyano; Mejía; Aguilar, 2023). Alongside the unplanned growth of cities, the context of climate change is noteworthy, bringing with it a range of potential environmental and socioeconomic impacts, including temperature elevation, shifts in precipitation patterns, and increased disease incidence (Erena et al., 2024; Salvador et al., 2024).

In Brazil, the semi-arid region is particularly vulnerable to unplanned urbanization and climate change (Mendes et al., 2020; Silva et al., 2024). According to Marengo (2016), the Brazilian semi-arid region is a high-risk area highly vulnerable to future climate changes, with an increased potential for disasters. Darela Filho et al. (2016) assess that the Brazilian semi-arid region exhibits medium to high vulnerability, coupled with a low capacity to implement public policies capable of adapting the region to climate change.

Temperatures in the Brazilian semi-arid region are predominantly high throughout the year, with minimums above 15ºC and maximums reaching up to 40ºC; rainfall is sparse and concentrated in short periods, with annual averages typically between 400mm and 650mm, concentrated in three or four months of the year, often in flash flood events that account for between 50% and occasionally 70% of the total annual precipitation (Jacomine, 1996; Tabarelli et al., 2018). Additionally, the geological formation and soils of the region are crystalline and shallow, directly influenced by the region's climate.

Several practices and tools are being studied and implemented to adapt vulnerable regions to climate change within the context of urban development. Monitoring the evolution of land use and occupation in areas undergoing human intervention and/or vulnerable to extreme weather events is essential for urban and environmental planning. Through this monitoring, it is possible to gather information on urban growth trends and their influence on surface runoff, determine soil infiltration capacity, assess environmental vulnerability, and establish relationships between changes in surface temperature and land use/cover (Valadares, 2017).

One way to monitor areas at local, regional, and global levels is through the use of Geographic Information Systems (GIS), which enable the integration of remote sensing and geoprocessing techniques. The use of GIS contributes to the organization, integration, identification, treatment, and processing of data from satellites and other remote sensing platforms, enabling a critical analysis of geographic space (Azevedo; Matias, 2024). With the increasing availability of medium and high-resolution satellite images, studies utilizing these products are becoming more common (Silva, Silva, Silva, 2016).

The municipality of Caruaru, located in the Agreste region of Pernambuco, is situated within the Brazilian semi-arid zone as defined by the Superintendence for the Development of the Northeast (SUDENE, 2017). Its characteristics include scarce rainfall, which is concentrated in a short period of the year and predominantly occurs in flash flood regimes (Medeiros; Holanda; França, 2024). Additionally, the municipality is characterized by shallow soils and the formation of watersheds with low concentration times, rendering the urban area vulnerable to adverse impacts during periods of intense precipitation events. Furthermore, the rapid population growth experienced by the municipality in recent decades has led to extensive urban development and, consequently, unplanned expansion of the urbanized area, including public roads.

Caruaru has experienced several flood events. In 2004, a major flood occurred, affecting 6 thousand people, resulting in 4 deaths, and causing estimated damages of 1 million reais, according to data from CPRM (2012). The record carried out by the Pernambuco Water and Climate Agency (APAC, 2022) in June 2022 pointed to a rainfall volume of approximately 40 mm in less than 24 hours, with this event causing numerous flooding points within the urban perimeter. As mentioned by CDAS (2017), intense rainfall occurred in the state of Pernambuco in 2017, causing 27 cities to declare a state of calamity due to floods, including Caruaru. The last flood event occurred on April 24, 2020, with 57 victims assisted by the Civil Defense. These occurrences highlight the urgent need to reconsider the urban drainage system as an essential infrastructure for mitigating damages caused by flooding and to consider urban stormwater management as a planning and management tool within the municipality.

Given this context, this study presents an analysis of land use and occupation evolution between the years 2000, 2015, and 2020 at a critical point with a history of flooding at the intersection of two important neighborhoods in Caruaru, using GIS tools. The objective of the study is to relate urban development and the evolution of land use and occupation with the potential generation of surface runoff and flood hydrographs, highlighting the impact of surface impermeabilization resulting from urbanization and providing information to define strategies aimed at addressing issues arising from unplanned urbanization coupled with extreme weather events.

Materials and methods

Study area

The study area is located in the city of Caruaru, situated in the Agreste Mesoregion and Vale do Ipojuca Microregion, in the state of Pernambuco, bordered to the north by Toritama, Vertentes, and Taquaritinga do Norte, to the south by Altinho and Agrestina, to the east by Bezerros and Riacho das Almas, and to the west by Brejo da Madre de Deus and São Caitano (Sousa et al., 2020). The territorial area of Caruaru covers 928.1 km², equivalent to 0.94% of the state, and is home to approximately 378,048 inhabitants (IBGE, 2024). Data from IBGE (2024) indicate that between 1991 and 2000, the population increased from 212,938 to 252,987 inhabitants. Between 2000 and 2010, the population grew from 252,987 to 314,912 inhabitants. From 1991 to 2000, Caruaru's population grew at an average rate of 1.93%, compared to 1.63% for Brazil as a whole. For the period from 2000 to 2010, Caruaru's population grew at an average annual rate of 2.21%, while in Brazil it was 1.17% during the same period (Figure 1).

The climate of Caruaru, according to the Köppen-Geiger classification, is semi-arid (Bsh), characterized by hot and dry summers and mild, rainy winters. Figure 1b presents the average rainfall values for Caruaru based on a 30-year historical series (APAC, 2024).

Caruaru is a medium-sized city with deficiencies in urban drainage planning and implementation. Urban planning instruments, such as the Municipal Master Plan established by Complementary Law No. 072, dated December 30, 2019, do not adequately address sustainable solutions for stormwater management and drainage issues. A survey conducted by the civil defense department for Caruaru identifies 433 points at risk of flooding and 4 points at risk of landslides (Figure 2).

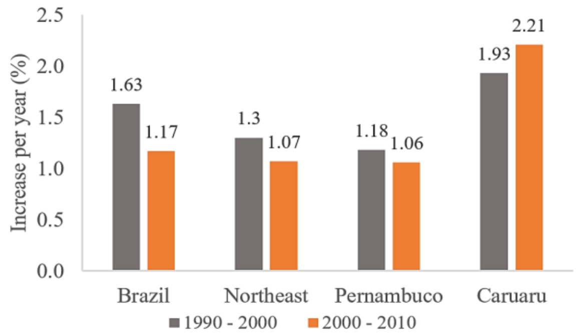

Figure 1. Annual population growth rate by geographical unit from 1911 to 2010.

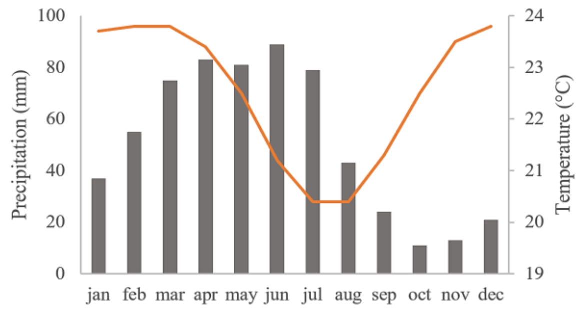

Figure 2. Rainfall and temperature based on a 30-year historical series.

Significantly, the neighborhoods of Maurício de Nassau and Universitário (also highlighted in Figure 3) are among the most valued areas of the city, characterized by high vertical development and extensive impermeabilization. Therefore, these neighborhoods have been selected as the study areas for this work.

Figure 4 shows the location of Caruaru and the selected study area, focusing on the critical flooding point identified by the Civil Defense in the Universitário neighborhood, near the border with Maurício de Nassau. The geographic coordinates of this point are 35.96635 latitude and -8.27426 longitude.

Once the study area and critical point were defined, the watershed contributing to the chosen critical point was delineated. To accomplish this, QGIS version 2.18.20 software was used along with TauDEM 5.1.2 algorithms. The input data consisted of Digital Terrain Models at a scale of 1:5,000 obtained from the Pernambuco Tridimensional (PE3D) database, a program by the state government of Pernambuco that conducted aerial photogrammetric coverage and generated orthophotos, laser profiling, and Digital Terrain Models (DTMs), Digital Elevation Models (DEMs), and Hypsometric Intensity images for the entire territory of the state of Pernambuco.

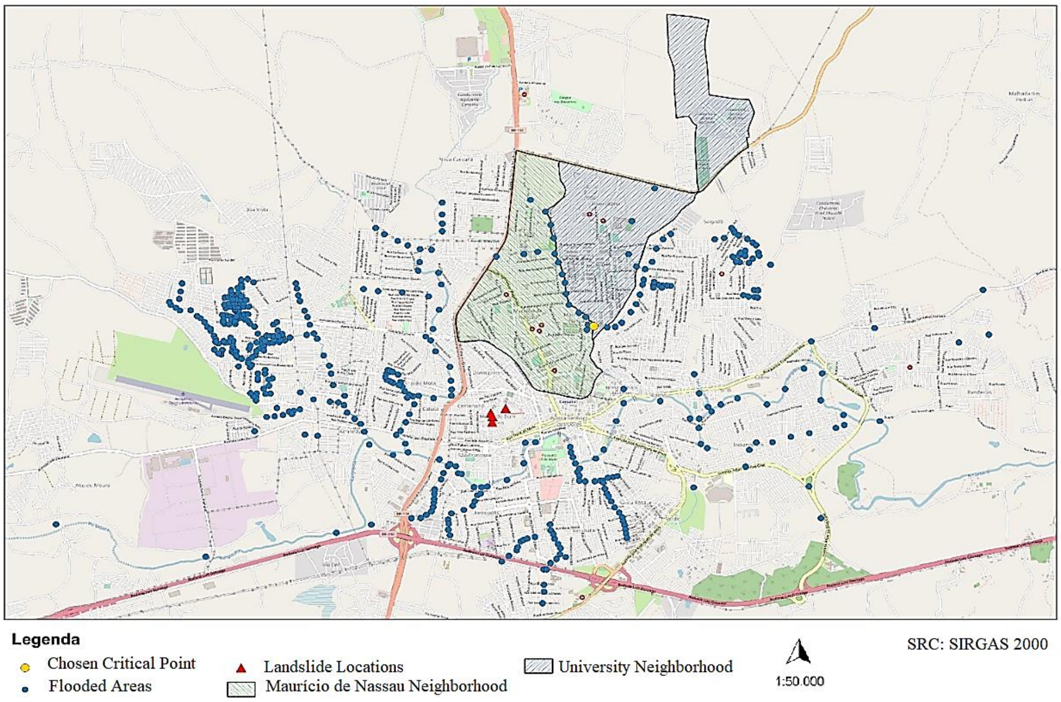

Figure 3. Points at risk of flooding and landslides identified by the Civil Defense of Caruaru.

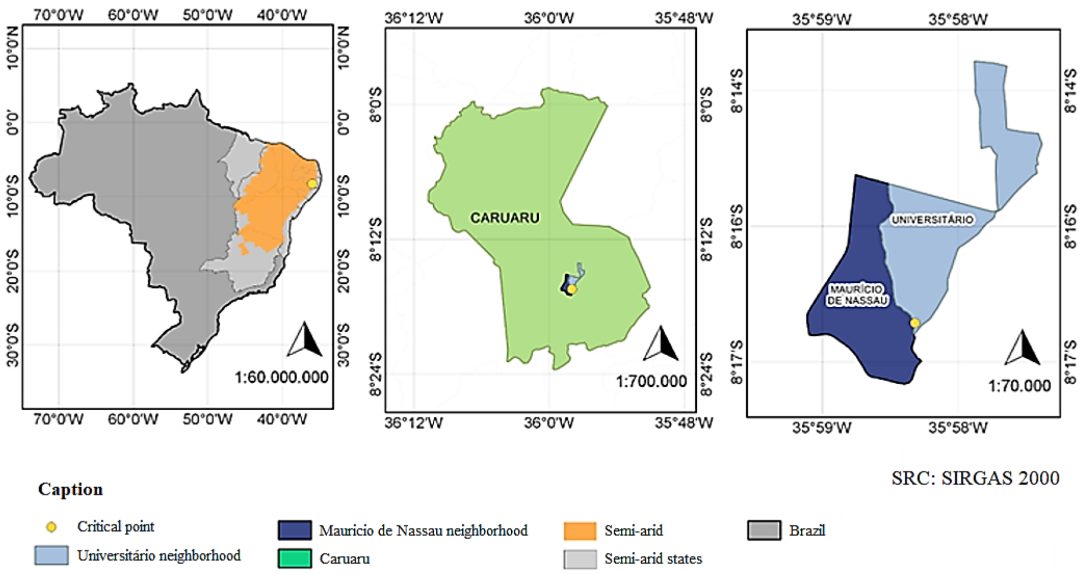

Figure 4. Points at risk of flooding and landslides identified by the Civil Defense of Caruaru.

The generated contributing watershed has an area of 3.707 km², comprising parts of the neighborhoods Luiz Gonzaga, Nova Caruaru, Maurício de Nassau, and Universitário, as observed in Figure 5.

The delineated area constitutes the physical system or water collection area for precipitation, which converges towards a single outlet section, known as the outlet. The hydrological response of a watershed is to transform a concentrated input of volume over time (precipitation) into a more distributed output of water (runoff) over time. Some watersheds are prone to floods and inundations. In such cases, it is necessary to develop control infrastructures based on the probability of occurrence of these events, such as designing hydraulic drainage structures like conduits, channels, culverts, etc., which are constructed based on the maximum design flow rate.

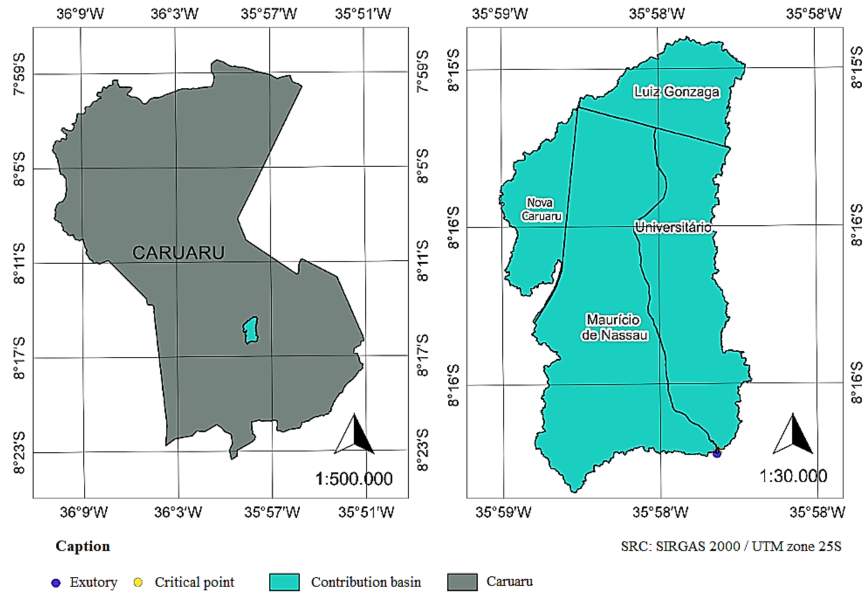

Figure 5. Generated contributing watershed with delineation of the neighborhoods it encompasses.

Estimation of peak flow using the rational method

The Rational method is one of the most commonly used methods for estimating runoff because it is older and more practical, requiring a small amount of information. This method encompasses all processes of transforming precipitation into runoff using just one coefficient (Froehlich, 2024; Sabzevari et al., 2024). The coefficient of runoff (C), also known as the runoff coefficient or coefficient of discharge, is defined as the ratio of the volume of surface runoff to the volume of precipitation, estimated based on the characteristics of the watershed. There are tables that relate the runoff coefficient to the nature of the surface where runoff occurs (Table 1).

Table 1. C coefficient values.

Surfaces	**C**
Perfect roofs, no leaks	0,70 a 0,95
Asphalt surfaces in good condition	0,85 a 0,90
Cobblestone, tile or wooden block paving with well-fitted joints	0,75 a 0,85
For previous surfaces without joints taken	0,50 a 0,70
Paving of lower blocks without the joints taken	0,40 a 0,50
Macadamized roads	0,25 a 0,60
Boulder roads and walks	0,15 a 0,30
Uncoated surfaces, railway yards and open land	0,10 a 0,30
Parks, gardens, lawns and meadows, depending on the slope of the soil and the nature of the subsoil	0,01 a 0,20

To obtain the value of the coefficient C for the watershed, surface classification was performed using the geoprocessing software eCognition Developer 64. Five thematic classes were generated: green area, impervious lot area, asphalt road, cobblestone road, and compacted soil. Initially, representative samples were collected for these created classes, followed by the classification of the total area of the watershed using the classification algorithm.

Surface classification was carried out using images from the contributing watershed of the year 2015 obtained from PE3D, as well as images from the years 2000 and 2020 obtained from Google Earth, which utilize satellite photographs from LANDSAT and Copernicus.

For the different types of land use, the coefficient C was calculated using Equation 1.

$$C_n = \frac{C_{n_1} \times A_1 + C_{n_2} \times A_2 + \cdots C_n \times A_n}{A_1 + A_2 + \cdots A_n} \qquad (1)$$

Where:
Cn: curve number coefficient for a specific surface;
An: area corresponding to that surface.

The equation of the Rational method is presented in Equation 2.

$$Q_{máx} = 0{,}278 \times C \times I \times A \qquad (2)$$

Where:
Q_{max}: maximum flow rate (m³/s);
C: runoff coefficient (dimensionless);
I: average precipitation intensity (mm/h);
A: watershed area (km²).

Estimation of the Hydrograph using the SCS Method

The Hydrograph using the SCS (Soil Conservation Service) Method is a widely used hydrological model for estimating surface runoff and peak discharge during precipitation events in watersheds. Developed by the USDA's Natural Resources Conservation Service, the SCS method uses empirical relationships between rainfall, land use, soil type, and land cover to predict the watershed's response. This model is especially useful in urban planning and water resource management, providing an essential tool for engineers and hydrologists in creating effective flood control and stormwater management systems (Li et al., 2023; Bai et al., 2024).

Commonly used for determining the design hydrograph, the SCS method assumes the following relationship as shown in Equation 3.

$$\frac{F_a}{S} = \frac{P_e}{P - I_a} \qquad (3)$$

Where:
P: precipitation (mm);
P_e: effective precipitation (mm);
F_a: height of precipitation retained in the watershed after the onset of surface runoff, representing continuous losses of precipitation (mm);
S: maximum potential retention (mm);
I_a: initial losses due to interception, depression storage, evapotranspiration, and infiltration prior to soil saturation (mm);
$P - I_a$: potential surface runoff (mm).

Assuming the hypothesis that the height of precipitation retained in the watershed after the onset of surface runoff is the difference between total precipitation and effective precipitation, we have Equation 4:

$$F_a = P - P_e \qquad (4)$$

The SCS assumes that initial losses are equal to 20% of the maximum water retention capacity in the watershed (Porto, 1995). Thus, the expression for calculating effective precipitation is obtained as Equation 5:

$$P_e = \frac{(P - 0{,}2S)^2}{(P + 0{,}8S)} \qquad (5)$$

It is worth noting that this equation is valid only for P>0.2S; otherwise, Pe=0. The maximum potential soil retention (S) is related to the curve number (CN), which represents the watershed's cover and soil conditions, by the following Equation 6.

$$S = \frac{25400}{CN} - 254 \qquad (6)$$

As presented, the values of CN are associated with the cover and soil conditions of the watershed. In this perspective, soils are grouped into four hydrological groups: A, B, C, and D (Table 2).

Table 3 provides estimated CN values for urban and suburban watersheds, categorized by each of the four hydrological soil groups.

Table 2. Hydrological Soil Groups.

Group	Types of soil and land use conditions
A	Sandy soils with low total clay content, less than 8%, without rocks or clay layers, or compacted layers down to a depth of 1.5 m. The humus content is very low, not reaching 1%. These soils generate low surface runoff and high infiltration.
B	Shallow sandy soils with higher clay content compared to Group A, but still less than 15%. There are no rocks or clay layers down to 1.5 m, although a denser layer beneath the surface layer is almost always present. These soils are less permeable than the previous group but still have above-average permeability.
C	Clayey soils with a total clay content of 20 to 30%, but without impermeable clay layers or containing rocks down to a depth of 1.2 m. In the case of "terra roxa" soils, these maximum limits can be 40% and 1.5 m. A denser layer is observed at about 60 cm depth compared to Group B soils, although still far from impermeable conditions.
D	Clayey soils (30 to 40% total clay) with a denser layer at about 50 cm depth. Alternatively, sandy soils like those in Group B but with an almost impermeable clay layer or layers of rounded pebbles. These soils have very low infiltration capacity, resulting in a higher proportion of surface runoff.

Table 3. Estimation of Curve Number Values for Urban and Suburban Watersheds.

Descrição do uso do solo		**Tipo de solo**			
		A	**B**	**C**	**D**
Espaços abertos: matos ou gramas cobrem 75% ou mais da área		39	61	74	80
Matos cobrem 50 a 75% da área		49	69	79	84
Áreas comerciais (85% impermeáveis)		89	92	94	95
Distritos industriais (72% impermeáveis)		81	88	91	93
Áreas residenciais		**Tipo de solo**			
Tamanho do lote (m²)	**Média da área impermeável (%)**	**A**	**B**	**C**	**D**
<500	65	77	85	90	92
1.000	38	61	75	83	87
1.300	30	57	72	81	86
2.000	25	54	70	80	85
4.000	20	51	68	79	84
Parques de estacionamentos, telhados, viadutos		98	98	98	98
Arruamentos e estradas: asfaltadas e com drenagem pluvial		98	98	98	98
Paralelepípedos		76	85	89	91
Terra		72	82	87	89

The soil in the studied watershed is classified as Planosol Haplic, categorized as Group D. This soil type is shallow, with a sandy and permeable texture, transitioning abruptly to a subsurface layer that is compacted and nearly impermeable. Its composition includes highly active clay, resulting in imperfect drainage and susceptibility to compaction (BRASIL, 1973; EMBRAPA 2018).

The SCS Unit Hydrograph

To convert design precipitation into streamflow in the watershed, it is necessary to apply a rainfall-runoff transformation model. The unit hydrograph method (HU) is an essential tool in hydrological analysis, allowing for an understanding of a watershed's response to precipitation (Ansori et al., 2022; Guo, 2023). It represents the watershed's response to a unit volume precipitation event of duration Δt through the unit hydrograph, which illustrates the variation of flow over time post-precipitation. This method is useful for estimating flow under different rainfall patterns and is valuable in modeling extreme events, flood prediction, and water resources management (Xu et al., 2023; Zhang et al., 2024).

The unit hydrograph can be determined based on the physical characteristics of the watershed. Figure 6 illustrates the parameters that characterize the unit hydrograph.

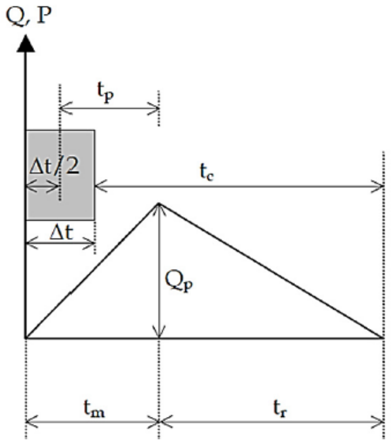

Figure 6. Triangular Unit Hydrograph (SCS).

These parameters are determined by first calculating the time of concentration (t_c) using the Kirpich method, given by Equation 7.

$$t_c = 0{,}95\left(\frac{L^3}{H}\right)^{0{,}385} \quad (7)$$

Where:
L: length of the main channel (km)
H: average slope of the main channel (m).

Subsequently, the parameter t_m is determined using Equation 8.

$$t_m = \frac{\Delta t}{2} + 0{,}6t_c \quad (8)$$

The peak time of the hydrograph (t_p) is then calculated using Equation 9.

$$t_p = 0{,}6t_c \quad (9)$$

The recession time of the hydrograph (t_r) is obtained using Equation 10.

$$t_r = 1{,}67t_p \quad (10)$$

The base time of the hydrograph (t_b) is also calculated using Equation 11.

$$t_b = t_m + t_r \quad (11)$$

Finally, the maximum flow rate (Q_p) is determined using Equation 12.

$$Q_p = \frac{0{,}208 \times A}{t_m} \quad (12)$$

The synthetic unit hydrograph of the SCS can be triangular or curvilinear. The curvilinear hydrograph provides higher accuracy compared to the triangular hydrograph. The curvilinear hydrograph is represented by the Gamma function (Equation 13), which was adopted by the SCS (WSDA, 1986):

$$\frac{q}{q_p} = \left[\frac{t}{t_p} \times \exp\left(1 - \frac{t}{t_p}\right)\right]^x \quad (13)$$

Where:
X: is given by the mathematical expression $0{,}8679 \times e^{(0{,}00353 \times PF)} - 1$;
PF: Typically adopted as 484.

The response of a watershed to a rainfall event depends on the physical characteristics of the watershed and the characteristics of the event, such as the duration and intensity of the rainfall. The duration of the considered rainfall event was equal to the time of concentration, 45 minutes, and the rainfall intensity was calculated using the Caruaru intensity-duration-frequency (IDF) equation obtained by Coutinho et al. (2013) (Equation 14). To use this equation, the duration intervals and return periods of 5 to 120 minutes and 2 to 100 years, respectively, must be respected.

$$i = \frac{228{,}02xTr^{0{,}2129}}{(t + 2{,}830777)^{0{,}558067}} \quad (14)$$

Where:
i: maximum average rainfall intensity (mm/h);
T_r: return period (years);
t: duration of rainfall (minutes).

Results and discussion

Determining the physical characteristics of the watershed

The contributing watershed and the flow network generated by TauDEM from the digital elevation model of the terrain are shown in Figure 7. The critical flooding point chosen and the watershed outlet are also identified in the image. The flow network helps identify the direction of flow.

Based on the digital terrain model, the contributing watershed covers a considerable area, totaling approximately 3,707 km². The definition of the critical point within the watershed was determined based on the identified flood-prone areas in the topography. This suggests that flood-prone locations were mapped and used as a reference for selecting the critical point. The topography plays a crucial role in this process, as it directly influences flow dynamics and water distribution in the watershed. Analyzing these flood-prone points along with the topography helps identify areas of risk and understand how water behaves within the watershed, which is essential for comprehending the inherent risks associated with irregular land use within the watershed.

In Table 4, a comprehensive overview of the physical characteristics of the contributing watershed is presented, including details such as total area, predominant topography, and hydrographic network. Additionally, the concentration time, calculated based on the Kirpich equation, is provided as a relevant indicator of the watershed's hydrological response. This concentration time is essential for understanding runoff dynamics and the watershed's response to precipitation events.

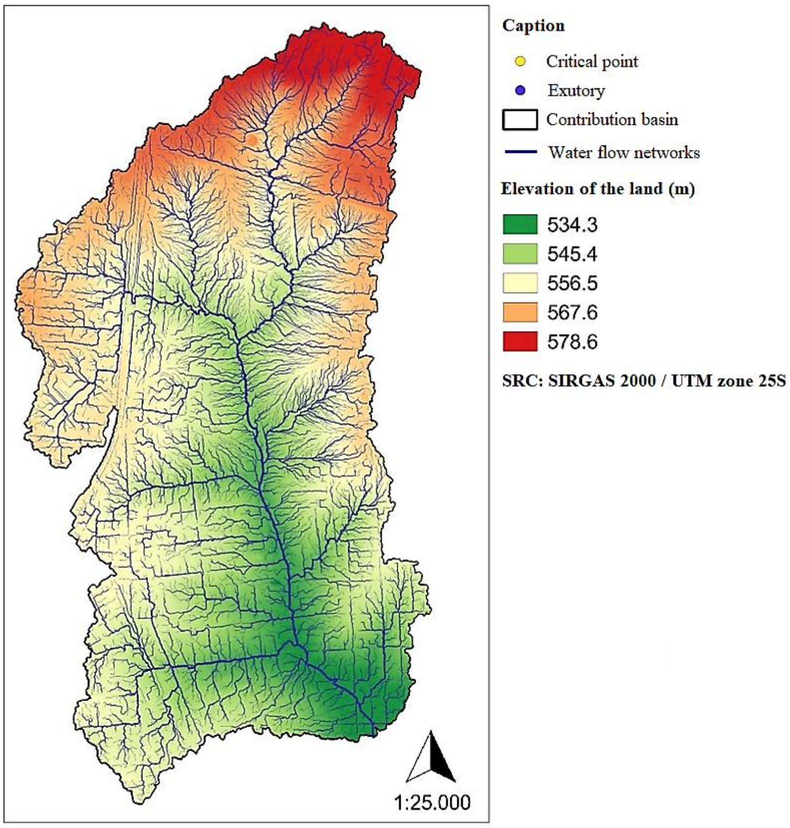

Figure 7. Flow networks of the contributing watershed.

Table 4. Physical characteristics of the basin and concentration time.

Characteristics	**Corresponding value**
Area (km²)	3,707
Length of the main watercourse (m)	2.124,80
Source quota (m)	543,99
Outflow quota (m)	527,05
Difference in level between the source and the outlet (m)	16,94
Concentration time (min)	45,79

Over time, significant changes in the watershed's landscape can be observed through remote sensing images, as detailed in Table 5, which compares watershed characteristics in the years 2000, 2015, and 2020. These images allow for an assessment of land use and land cover evolution, providing valuable insights into environmental and developmental trends over time.

The classification of these images into five distinct thematic classes (green area, impervious area of lots, asphalt roads, cobblestone roads, and compacted soil) was performed to generate detailed land use and land cover maps, as presented in Table 6. These maps are crucial for identifying urbanization patterns, urban expansion, and changes in vegetation cover within the watershed over the analyzed period. Understanding these changes is fundamental for environmental planning and sustainable water resource management within the study area. The land use and land cover classification data reveal significant changes in the landscape of the watershed over the past two decades.

The green area, consisting of natural vegetation and open spaces, experienced a substantial decrease from 26% of the total area in 2000 to just 6% in 2020. This reduction indicates intense urban pressure and increased urbanization within the contributing watershed.

Conversely, the impermeable area of lots, representing urban and built-up areas, saw a notable increase from 25% in 2000 to 44% in 2020. This reflects urban expansion and infrastructure development over time, leading to greater soil impermeability and altering the natural drainage pattern.

Areas occupied by asphalt and cobblestone roads showed relatively modest changes, with proportions increasing marginally over the two decades. The slight variations in these categories indicate relative stability in road infrastructure within the watershed.

Table 5. Images of the contribution basin.

Year 2000	**Year 2015**	**Year 2020**
 SRC: SIRGAS 2000 / UTM zone 25S		 1:37.000

Table 6. Classified images of the catchment area.

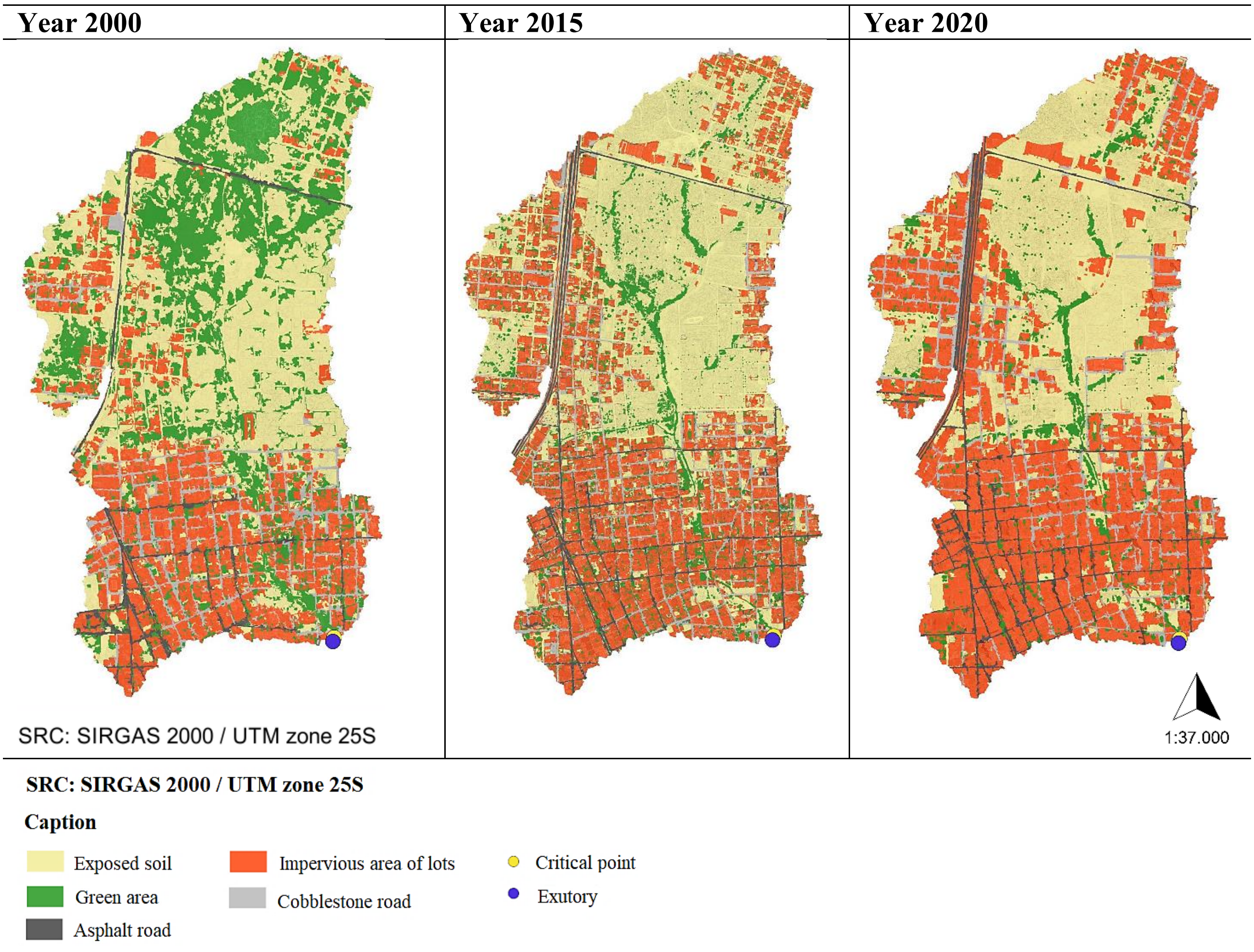

Finally, the exposed soil area exhibited fluctuations over the analyzed period, initially increasing between 2000 and 2015, followed by a reduction between 2015 and 2020. These changes are likely related to vegetation removal and residential development in previously unoccupied areas.

The data displayed in Table 7 and illustrated in Figure 8 present, in square kilometers, the evolution of each category of area, indicating an understanding of the impacts of urbanization in the specific river basin and highlighting the importance of sustainable land use and management of natural resources in this context.

Table 7. Class area in km² for the years studied.

Classes	Year 2000	Year 2015	Year 2020
Green area	0,966	0,333	0,225
Asphalt road	0,111	0,177	0,185
Impervious Area of Lots	0,934	1,32	1,620
Exposed Soil	1,468	1,609	1,400
Cobblestone Road	0,228	0,268	0,277
Total	3,707	3,707	3,707

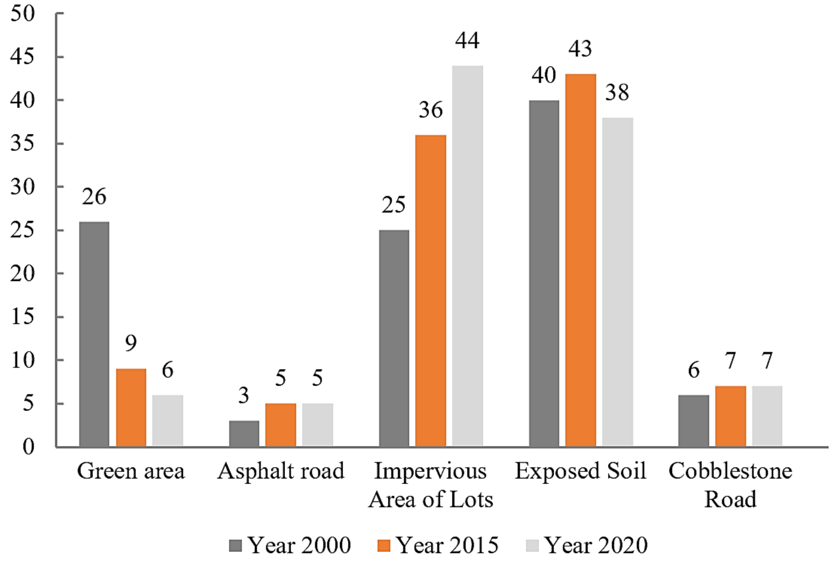

Figure 8. Class area in % for the years studied.

The determination of maximum flow for different rainfall return periods (TR) using the rational method is fundamental to assess surface runoff potential and flood risks in the watershed over time. The results reveal a significant increase in maximum flow over the years studied. Between 2000 and 2015, there was a 26% increase in maximum flow, indicating a greater hydrological response of the watershed to precipitation events during this period (Table 8). This increase can be attributed to changes in land use, such as increased surface sealing due to urban development and expansion of built-up areas.

Table 8. Maximum flow by the Rational Method in m³/s for the years and TR studied.

Return Period (years)	**Year 2000**	**Year 2015**	**Year 2020**
TR 2 years	12.44	15.71	17.55
TR 10 years	17.53	22.13	24.72
TR 25 years	21.31	26.89	30.04
TR 50 years	24.69	31.17	34.82
TR 100 years	28.62	36.12	40.35

Even more alarming is the 41% increase in maximum flow between 2000 and 2020. This substantial increase suggests an intensification of hydrological impacts of urbanization over the past two decades. The coefficient of surface runoff (C), which represents the fraction of rainfall that becomes surface runoff, also increased over the period, from 0.40 in 2000 to 0.56 in 2020. This increase in C is directly linked to the increased soil sealing and growth of urban areas in the watershed.

The SCS (Soil Conservation Service) triangular and curvilinear unit hydrograph for the studied watershed, as presented in Figure 9, provides crucial insights into the hydrological response of the area to precipitation events. The unit hydrograph is a graphical representation of the watershed's response to a unit of rainfall, showing the temporal distribution of resulting flow. The observed peak flow was 1.53 $m^3/s/mm$, meaning that for every millimeter of rainfall on the watershed, the maximum instantaneous flow reaches 1.53 cubic meters per second. Furthermore, this peak flow occurred within a short period of time, specifically at 0.50 hours (or 30 minutes) after the onset of rainfall. These data are essential for designing flood control structures and understanding watershed hydrodynamics, aiding in water resources planning and management to mitigate flood and erosion risks.

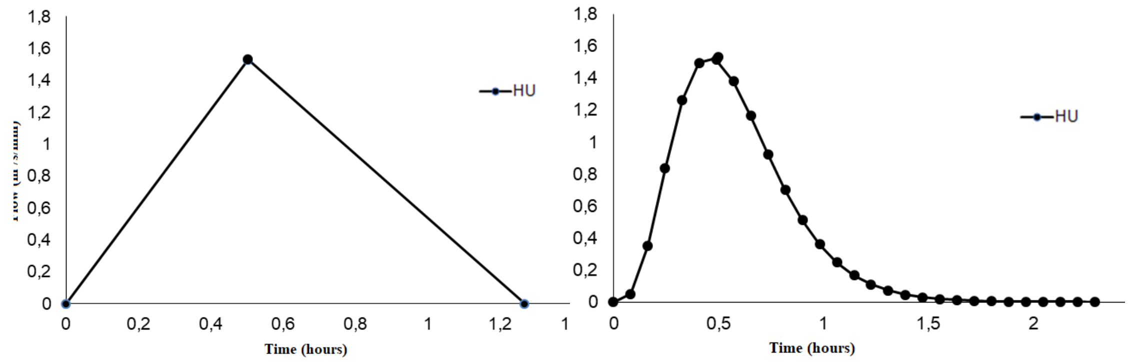

(a) (b)

Figura 9. SCS unit hydrograph for contribution basin: (a) triangular; (b) circular.

Conclusions

Based on the obtained results, the analysis of land surface cover, quantified by the studied classes, demonstrates that the urbanization process of the watershed results in a significant reduction of green areas and a nearly proportional increase in impermeable lot areas, due to the occupation of previously unoccupied areas and the consequent removal of vegetation cover. The simulations performed to determine peak flows reveal that surface alterations due to urban concentration have a substantial influence on the increase in these flows.

This trend of urbanization, characterized by the replacement of natural areas with impermeable structures such as pavements and buildings, drastically alters the hydrological balance of the watershed. The decrease in permeable areas limits water infiltration into the soil, increasing the volume of surface runoff, which can exacerbate flooding problems and overload urban drainage systems. Thus, changes in land use driven by urban growth have direct implications for water management and environmental sustainability in the affected regions.

The characterization of the watershed soils using C and CN coefficients, facilitated by Geographic Information Systems (GIS) and the increasing availability of medium and high-resolution satellite images, proves to be a valuable tool for the quantitative and qualitative monitoring of land use and its impact on surface runoff and soil infiltration capacity. The use of GIS allows for a more precise and detailed analysis of changes in land cover, providing a solid foundation for decision-making in urban and environmental planning.

In conclusion, this study underscores the urgent need for public policies that consider the hydrological impacts of urbanization. The integration of technological tools such as GIS and satellite imagery into urban planning and management is crucial for promoting sustainable development. Awareness of the importance of maintaining green areas and adequately managing surface runoff is fundamental to mitigating the adverse effects of urbanization and ensuring the resilience of urban watersheds.

Acknowledgments

The authors extend their sincere gratitude to the Coordination for the Improvement of Higher Education Personnel (CAPES) for the financial support provided through a doctoral scholarship under Process Nº. 88887.807916/2023-00, and for additional financial support granted through Process Nº. 88887.689130/2022-00. We also wish to thank the Fundação de Amparo à Ciência e Tecnologia de Pernambuco (FACEPE) for their financial support provided through Projects APQ-1767-3.01/22 and APQ-1535-3.01/22.

References

Ahmed, N., Luqman, M., 2024. Explaining urban communities' adaptation strategies for climate change risk: novel evidence from Rawalpindi, Pakistan. Natural Hazards [Online]. Available: https://doi.org/10.1007/s11069-024-06501-8. Accessed: 08 may. 2024.

Alves, P. B. R., Rufino, I. A. A., Feitosa, P. H. C., Djordjević, S., Javadi, A., 2020. Land-Use and Legislation-Based Methodology for the Implementation of Sustainable Drainage Systems in the Semi-Arid Region of Brazil. Sustainability [Online] 12. Available: https://doi.org/10.3390/su12020661. Accessed: 10 may. 2024.

Ansori, F. B., Lasminto, U., Kartika, A. A. G., 2023. Flood hydrograph analysis using synthetic unit hydrograph, hec-hms, and HEC-RAS 2D unsteady flow precipitation on-grid model for disaster risk mitigation. International Journal of GEOMATE [Online] 25. Available: https://doi.org/10.21660/2023.107.3719. Accessed: 12 may. 2024.

APAC. Agência Pernambucana de Águas e Clima, 2022. Aviso meteorológico N° 53/2022. Recife.

APAC. Agência Pernambucana de Águas e Clima, 2024. Climatologia – Precipitação média por município. Recife.

Azevedo, T., Matias, L. F., 2023. Urban land use and land cover mapping: proposal of a classification system with remote sensing. Landscape Geography [Online] 23. Available: https://orcid.org/0000-0003-3331-9176. Accessed: 05 may. 2024.

Bai, J., Li, J., Ran, H., Zhou, Z., Dang, H., Zhang, C., Yu, Y., 2024. Influence of varied drought types on soil conservation service within the framework of climate change: insights from the Jinghe River Basin, China. Journal of Arid Land [Online] 16. Available: https://doi.org/10.1007/s40333-024-0070-7. Accessed: 06 may. 2024.

Campos, J. N. B., Studart, T. M. C., 2008. Drought and water policies in Northeast Brazil: Backgrounds and rationale. Water Policy [Online] 10. Available: https://doi.org/10.2166/wp.2008.058. Accessed: 09 may. 2024.

Cardoso, M. R. D., Marcuzzo, F. F. N., Barros, J. R., 2014. Classificação climática de Köppen-Geiger para o estado de Goiás e o Distrito Federal. ACTA Geográfica [Online] 8. Available: https://doi.org/10.5654/actageo2014.0004.0016. Accessed: 11 may. 2024.

CDAS. Centro de Desenvolvimento Agroecológico Sabiá, 2017. Enchentes na Zona da Mata de Pernambuco: tragédia anunciada. Recife.

Coutinho, A. P., Leite, L. L. L., Ribas, L. V., Antonino, A. C. D., Cabral, J. J. S. P., Montenegro, S. M. G. L., 2013. Coletânia de equações de chuvas intensas para o estado de Pernambuco. XX Simpósio Brasileiro de Recursos Hídricos. Available: https://abrh.s3.sa-east-1.amazonaws.com/Sumarios/155/c82d638c1a944273d6e48f82daccc54c_384c7bf2fd51c1d8f781dbd4f8152a4b.pdf. Accessed: 02 may. 2024.

CPRM. Companhia de Pesquisa de Recursos Minerais, 2012. Ação emergencial para reconhecimento de áreas de alto e muito alto risco a movimentos de massas e inundações: Caruaru, PE. Caruaru.

Darela Filho, J. P., Lapola, D. M., Torres, R. R., Lemos, M. C., 2016. Socio-climatic hotspots in Brazil: how do changes driven by the new set of IPCC climatic projections affect their relevance for policy?. Climatic Change [Online] 136. Available: https://doi.org/10.1007/s10584-016-1635-z. Accessed: 10 may. 2024.

EMBRAPA. Empresa Brasileira de Pesquisa Agropecuária, 2012. Boletim de Pesquisa e Desenvolvimento: Climatologia do Estado de Alagoas. Recife.

EMBRAPA. Empresa Brasileira de Pesquisa Agropecuária, 2018. Sistema Brasileiro de Classificação de Solos. Brasília.

Erena, S. H., Reddy, R. U., Wodnimu, M. A., Mohamed, A., 2024. Flood vulnerability mapping and local mitigation strategies: The case of Adama City, Ethiopia. Urban Climate [Online] 55. Available: https://doi.org/10.1016/j.uclim.2024.101906. Accessed: 11 may. 2024.

Ferraz, C. M. L., Valadão, R. C., Pinto, D. B. F., Almeida, R. A., 2022. Inundações e alagamentos em Teófilo Otoni, Minas Gerais, Brasil, segundo indicadores geomorfológicos. Revista Brasileira de Geomorfologia [Online] 23. Available: http://dx.doi.org/10.20502/rbg.v23i4.2152. Accessed: 12 may. 2024.

Froehlich, D. C., A Modified Rational Method Approach for Calculating First Flush Design Flow Rates to Mitigate Nonpoint Source Pollution from Stormwater Runoff. Hydrology [Online] 11. Available: https://doi.org/10.3390/hydrology11020021. Accessed: 14 may. 2024.

Guo, J., 2023. Design Hydrographs in Small Watersheds from General Unit Hydrograph Model and NRCS-NOAA Rainfall Distributions. Journal of Hydrologic Engineering [Online] 28. Available: https://doi.org/10.1061/JHYEFF.HEENG-59. Accessed: 11 may. 2024.

IBGE. Instituto Brasileiro de Geografia e Estatística, 2023. Panorama – Caruaru, Pernambuco. Brasília.

IBt. Instituto de Botânica, 2010. Águas do Brasil: análises estratégicas. São Paulo.

Li, C., Lu, T., Wang, S., Xu, J., 2023. Coupled Thorens and Soil Conservation Service Models for Soil Erosion Assessment in a Loess Plateau Watershed, China. Remote Sensing [Online] 15. Available: https://doi.org/10.3390/rs15030803. Accessed: 10 may. 2024.

MAPA. Ministério da Agricultura, Pecuária e Abastecimento, 1973. Levantamento exploratório – reconhecimento de solos do estado de Pernambuco. Recife.

Marengo, J. A., Cunha, A. P., Alves, L. M., 2016. A seca de 2012-15 no semiárido do Nordeste do Brasil no contexto histórico. Revista Climanálise [Online] 3. Available: http://climanalise.cptec.inpe.br/~rclimanl/revista/. Accessed: 11 may. 2024.

Medeiros, R. M., Holanda, R. M., França, M. V., 2021. Caruaru - PE, your comfort or thermal discomfort in years of el niño, la niña. Revista Mirante [Online] 14. Available: https://www.revista.ueg.br/index.php/mirante/article/view/11834/8369. Accessed: 11 may. 2024.

Menezes, J. P. C., Bittencourt, R. P., Farias, M. S., Bello, I. P., Fia, R., Oliveira, L. F. C., 2016. Relação entre padrões de uso e ocupação do solo e qualidade da água em uma bacia hidrográfica urbana. Engenharia Ambiental e Sanitária [Online] 21. Available: https://doi.org/10.1590/S1413-1522016145405. Accessed: 12 may. 2024.

Moyano, S. C., Mejía, P. J. C., Aguilar, E. O. E., 2023. Patrones de asentamiento en la inundación pluvial del núcleo metropolitano de una ciudad al norte del Perú. Revista Geográfica de Chile Terra Australis [Online] 59. Available: https://doi.org/10.23854/07199562.2023591.escalona. Accessed: 08 may. 2024.

Nóbrega, R. S., Farias, R. F. de L., Santos, C. A. C. S., 2015. Variabilidade temporal e espacial da precipitação pluviométrica em Pernambuco através de índices de extremos climáticos. Revista Brasileira de Meteorologia [Online] 30. Available: https://doi.org/10.1590/0102-778620130624. Accessed: 08 may. 2024.

Peel, M. C., Finlayson, B. L., McMahon, T. A., 2007. Updated world map of the Köppen-Geiger climate classification. Earth System Science [Online] 11. Available: https://doi.org/10.5194/hess-11-1633-2007. Accessed: 11 may. 2024.

Pereira, L. S., Angelini, L. P., Danelichen, V. H. M., Gomes, L. F., 2024. Space-time evaluation of the transformation of land use and occupation and its impacts on surface temperature in Rio Verde - GO. Revista Brasileira de Geografia Física [Online] 17. Available: https://doi.org/10.26848/rbgf.v17.1.p494-507. Accessed: 12 may. 2024.

Porto, R. L. L., 1995. Escoamento superficial direto. In Drenagem Urbana. Porto Alegre: Abrh/Editora da Universidade/Ufrgs.

Sabzevari, T., Haghighi, A. T., Ghadampour, Z., Petroselli, A., Namazi, H., 2024. Estimation of Regional Design Runof Coefcient in the Rational Method. Iranian Journal of Science and Technology [Online] 48. Available: https://doi.org/10.1007/s40996-023-01286-5. Accessed: 11 may. 2024.

Salvador, M. S. S., Lucena, D. B., Souza, B. I., Sampaio, T. V. M., Borges Neto, I. I., 2024. Trends of climatic elements in the Semi-arid Region of Brazil: Case study of Cariri paraibano. RA'EGA [Online] 59. Available: http://dx.doi.org/10.5380/raega.v59i0.94992. Accessed: 12 may. 2024.

SDEC. Secretaria de Desenvolvimento Econômico do Estado de Pernambuco, 2016. Pernambuco Tridimensional. Recife.

Silva, J. N. B., Galvíncio, J. D., Miranda, R. Q., Moura, M. S. B., 2024. Estimativa temporal e espacial do desempenho dos modelos de regressão calibrados para os fluxos de carbono em área de floresta tropical sazonalmente seca de caatinga. Revista da Casa de Geografia de Sobral [Online] 26. Available: https://doi.org/10.35701/rcgs.v26.975. Accessed: 05 may. 2024.

Silva, J. S. S., Silva, R. M., Silva, A. M., 2016. Mudanças do uso e ocupação do solo e degradação eco-ambiental usando imagens orbitais: o estudo de caso da bacia do rio Bacanga, São Luís (MA). Revista Brasileira de Geografia Física [Online] 9. Available: https://doi.org/10.26848/rbgf.v9.1.p265-279. Accessed: 14 may. 2024.

SUDENE. Superintendência de Desenvolvimento do Nordeste, 2017. Resolução N° 107/2017 - Estabelece critérios técnicos e científicos para delimitação do Semiárido Brasileiro e procedimentos para revisão de sua abrangência. Brasília.

WSDA. Washington State Department of Agriculture, 1986. Urban hidrology for smail watersheds. Washington.

Xu, Y., Liu, C., Yu, Q., Zhao, C., Quan, L., Hu, C., 2023. Study on a Hybrid Hydrological Forecasting Model SCE-GUH by Coupling SCE-UA Optimization Algorithm and General Unit Hydrograph. Water [Online] 15. Available: https://doi.org/10.3390/w15152783. Accessed: 14 may. 2024.

Zhang, L., Xu, W., Zhang, F., Zhang. W., Wei, W., Zhang, X., 2024. Improved general unit hydrograph model for dam-break flood hydrograph. Journal of Hydrology [Online] 635. Available: https://doi.org/10.1016/j.jhydrol.2024.131216. Accessed: 11 may. 2024.